Aalborg Universitet

AALBORG UNIVERSITY
DENMARK

A Review of Traditional Helical to Recent Miniaturized Printed-Circuit-Board Rogowski Coils for Power Electronic Applications

Shi, Yafei; Xin, Zhen; Loh, Poh Chiang; Blaabjerg, Frede

A Review of Traditional Helical to Recent Miniaturized Printed Circuit Board Rogowski Coils for Power-Electronic Applications

Yafei Shi , *Student Member, IEEE*, Zhen Xin , *Member, IEEE*, Poh Chiang Loh, and Frede Blaabjerg , *Fellow, IEEE*

Abstract—Latest wide-bandgap power devices are switching progressively faster compared with existing silicon devices. Their accurate current measurements for either control or protection have therefore become tougher. One method that can fulfill the requirements is to use a Rogowski coil and its accompanied electronics to form a Rogowski current sensor with high bandwidth, small volume, low cost, and ease of integration. This article therefore aims to review various aspects of the Rogowski current sensor from its history, measuring principles to modern power-electronic applications. The applications have, in turn, motivated a progression from traditional helical to recent miniaturized printed circuit board implementation, in order to improve the overall power density. This progression has similarly been reviewed, together with its various design aspects applied to the winding, integrator, shielding, and parameters of the Rogowski current sensor. Future challenges and directions are then summarized, whose ultimate goal is to maximize accuracy over a wide bandwidth without being affected by radiated and near-field-coupling interferences.

Index Terms—Current sensor, printed circuit board (PCB), Rogowski coil, wide-bandgap semiconductor, wide bandwidth.

I. INTRODUCTION

CURRENT sensors have been widely used for measuring currents of components and systems for either control or protection [1]. They are usually of different types, depending on the requirements of the considered applications. Commonly stated requirements are high accuracy, low power consumption, low cost, small volume, or a combination of them [2]. Moreover, in a power-electronic system, some current sensors are for

measuring currents of power devices, which increasingly may be fabricated with silicon carbide (SiC) and/or gallium nitride (GaN). Such newer semiconductors can operate with previously unattainable switching frequencies, which in turn, can shrink the sizes of passive components. The high switching frequencies have however created a challenge for the current-sensing bandwidth. For example, with the SiC device C2M0080120D from *CREE*, its rise time T_r is 20 ns [3] and its minimum bandwidth BW is 17.5 MHz, according to $\mathrm{BW} = 0.35/T_r$. Its current-sensing bandwidth must hence be three to five times bigger than BW or 52–88 MHz, to guarantee sufficient accuracy [4].

Current sensors for newer semiconductors must hence be improved while not adding too much volume to the desirably compact system. Existing current sensors cannot meet the requirements, since they are mostly large, expensive, limited in bandwidth, and/or at times, introduce nonnegligible insertion impedances in series with the semiconductors. These limitations, associated with some common current sensors such as current transformer (CT), shunt, Hall-effect sensor, and Rogowski coil, are better described, as in the following.

Beginning with CT, its accuracy is satisfactory and its bandwidth can be as high as tens of MHz for ac current sensing only (cannot measure dc) [5]. However, it suffers from possible flux saturation and size limitations, which immediately render it not suitable for a compact power-electronic system. The shunt can then be considered, especially if both ac and dc currents must be measured. Its principle is based on simple resistive voltage divider, after being inserted into the current loop. However, its resistive skin effect and presence of self-inductance seriously affect its accuracy at high frequencies [6]. Coaxial shunt must hence be chosen to reduce skin effect, whereas thinner conductor with a higher resistivity and no magnetic field space within it must be chosen to reduce self-inductance [7]. Coaxial shunt can additionally introduce a gigahertz bandwidth [8], but its large volume and expensiveness normally limit its wide usage.

The next option is then to try the Hall-effect sensor, which presently is the most popular current sensor with a magnetic field. The Hall sensor can favorably measure dc current, but its bandwidth is normally less than 1 MHz, in order to avoid overheating caused by core losses [5]. Its measuring range is also limited by possible core saturation, which frequently will introduce an unintended output offset [2]. Accuracy of the Hall

TABLE I
COMPARISON OF EXISTING CURRENT SENSORS [2], [5]–[11]

	Range	Bandwidth	DC	Isolated	Saturation	Size	Cost
CT	A-kA	kHz-MHz	No	Yes	Yes	Large	Medium
Shunt	kA	kHz-MHz	Yes	No	No	Small	Low
Coaxial Shunt	mA-A	GHz	Yes	No	No	Large	High
Hall	A-kA	kHz	Yes	Yes	Yes	Medium	High
Rogowski	A-MA	kHz-MHz	No	Yes	No	Small	Low

sensor has hence been compromised. This, together with its larger size and expensiveness, has rendered it not ideal for wide-bandgap devices. A better option is thus to consider the Rogowski coil, whose bandwidth can be as wide as 1 GHz [9]. This is possible because each Rogowski coil is an inexpensive air-coil without a magnetic core [10]. It thus does not experience magnetic saturation and can be made promisingly small for integration within a power-electronic system [11]. This, together with its other characteristics and those of alternative current sensors mentioned above, is summarized in Table I.

Lately, implementation of a Rogowski coil has also evolved from its traditional helical to its newer printed circuit board (PCB) type for closer integration with discrete devices or modules. This evolution, together with various design aspects of a Rogowski coil, is now reviewed with focus directed mainly at power-electronic systems. Its intention is to provide readers with a general understanding of high-bandwidth current measurement offered by a Rogowski coil and its PCB implementation. Section II therefore systematically starts by providing a history of Rogowski coil and its possible types organized in terms of how its winding and core have been implemented. Section III then describes how a Rogowski coil can function as a current sensor, its accompanied components, and electromagnetic interferences that can alter its measurement accuracy. This is followed by Sections IV and V, which describe how winding and shielding features can be transferred from traditional helical to PCB Rogowski coil.

Other necessities like prospective integrators and coil modeling techniques are then described in Sections VI and VII, which together with earlier sections complete the theoretical background of Rogowski current measurement. Its existing applications and future challenges are eventually described in Sections VIII and IX. Finally, Section X concludes this article.

II. HISTORY AND TYPES OF ROGOWSKI COILS

Over a hundred years ago, in 1912, W. Rogowski and W. Steinhaus coauthored a paper named "Die Messung der Magneticschen Spannung," where they described a coil wound on a flexible nonmagnetic strip [12]. They then performed several experiments with the coil for measuring an electric current. The coil was later named as Rogowski coil. Equivalent measurement had, in fact, also been documented even earlier in an article titled "On a Magnetic Potentiometer" written by A. P. Chattock in 1887. In it, Chattock [13] demonstrated how a long flexible coil could be used for measuring magnetic potential, induced by an electric current, across terminals of the coil. Since then, several usages of Rogowski coil have surfaced in laboratories for specialized electronic current measurements needed by a wide

range of applications. Each usage may however adopt a different implementation for its winding and skeleton (or air core), which broadly can be classified as follows.

A. Flexible Winding on Flexible Skeleton

This is the most widely found type, implemented with both flexible winding and flexible rectangular or circular skeleton [14]. Although the resultant flexible helical (with circular skeleton) coil is convenient for probing a power-electronic system, it has some unresolved disadvantages. One of which is its difficulty to ensure evenness of its winding turns. The outcome is a slight degradation of measurement accuracy, which may not suit all practical applications.

B. Rigid Winding on Rigid Skeleton

This type of coil is realized through routing a rectangular winding with traces and vias within a rigid PCB. It can thus be referred to as a PCB Rogowski coil, which according to the timeline, can be viewed as a progression of flexible helical Rogowski coil. Its purpose is to reduce the size of the coil for easier integration within a highly dense power-electronic system. Being small also helps it to reduce stray reactance, and hence widen its bandwidth, as explained in a later section. Moreover, as a PCB, its design can be computerized and checked with a computer-aided design software, such as *Altium Designer*, *ORCAD*, *PADS*, and *EAGLE* to name only a few. This, together with its accompanied manufacturing precision and automation, can help to lower cost, and guarantee uniformity and consistent performances among multiple produced coils [15], [16]. PCB Rogowski coil thus has promising prospects, especially for power-electronic systems, where it has been used for measuring current through an Si, SiC, or GaN power device and/or an electrolytic capacitor. The accurately measured current over a wide bandwidth can then be used for short-circuit protection or lifespan monitoring.

C. Rigid Winding on Flexible Skeleton

The winding for this type of Rogowski coil is again formed by conductive traces and vias [17], but instead of a rigid PCB, it is printed on a flexible PCB [18], which hence constitutes a flexible skeleton. The printed winding is however rigid, since it cannot move with respect to the skeleton, even though the resulting PCB Rogowski coil is overall flexible. The resulting coil also has good sensitivity, but it is not popularly suitable for power electronics due to its typically higher cost than a rigid PCB Rogowski coil.

III. ROGOWSKI COIL AS CURRENT SENSOR

A. Operating Principles

Regardless of its type, a Rogowski coil is for measuring an alternating current using a winding on an air core. Its operating principles are similar to those of a CT based on Faraday's law [10]. To illustrate, Fig. 1 shows a simple schematic, where current $i_1(t)$ to be measured is in the primary conductor. This
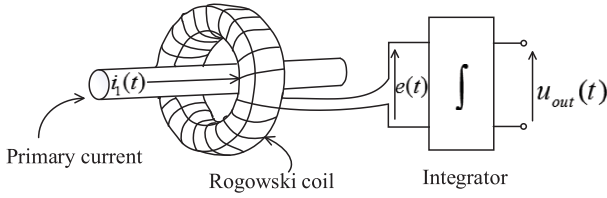
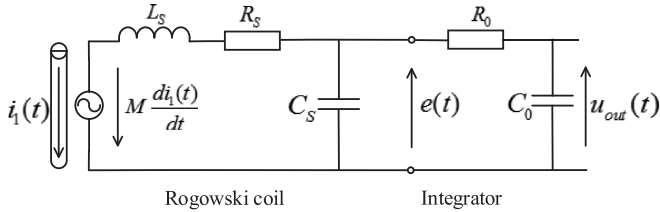Fig. 1.   Sketch of a Rogowski current sensor.

Fig. 2.   Equivalent circuit of a Rogowski coil and an integrator.

current causes magnetic fluxes to circulate around the conductor with some of them linking the secondary Rogowski coil. An induced voltage, according to (1), can then be detected across the coil

$$u_s(t) = \frac{d\phi}{dt} = M\frac{di_1}{dt} \tag{1}$$

where M is the mutual inductance of the coil, and di_1/dt is the rate of change of the primary current [19].

The induced voltage, upon integrated as in Fig. 1, then gives a scaled $i_1(t)$ for measurement. Operating principles of a Rogowski coil are thus comparably simple, from which it can be concluded too that the coil cannot measure dc current with zero derivative. This problem can however be solved by including a complementary sensor, such as a Hall-effect sensor, to be discussed in Section IX-C. Meanwhile, without a magnetic core, Rogowski coil does not experience flux saturation, and can hence better sense a high-frequency ac current, whose derivative increases with frequency. It is thus an appropriate sensor for sensing current through a fast-switching power device, especially after being miniaturized into a PCB.

B. Coil Model

Before manufacturing, it is helpful to have a model for accurately predicting bandwidth and other characteristic parameters of the coil. The simplest of which is probably the circuit shown in Fig. 2, consisting of an ohmic resistance R_S, a self-inductance L_S, an induced voltage determined by mutual inductance M, and a lumped capacitance C_S for representing multiple parasitic capacitances between turns of the coil (does not include capacitive coupling with noise sources external of the coil). Expressions for these parameters are given in Section VII, which upon computed give L_S and C_S values for finding resonance frequency and hence bandwidth of the coil [20], [21]. More clearly, its piecewise linear magnitude response has been drawn in Fig. 3(a) for showing how its gain rises until resonance frequency f_H. After this, it begins to roll back, which is caused mainly by practical imperfections. Appropriate design of the

coil dimensions is thus important, in order to get satisfactory L_S, C_S, and hence f_H.

C. Integrator Model

A passive or an active integrator after the coil is necessary for reconstructing a scaled primary current for measurement. In Fig. 2, a passive *RC* integrator has been shown as an example [22], whose magnitude response in Fig. 3(b) obviously resembles a low-pass filter with integral characteristic at higher frequencies. This response, when combined with that of the coil in Fig. 3(a), gives the bandpass characteristic in Fig. 3(c) for representing the final current sensor. The figure also indicates that low and high cutoff frequencies, f_L and f_H, of the sensor are decided by the integrator and coil, respectively [23].

D. Electromagnetic Interferences

When used as a current sensor in practice, both Rogowski coil and its integrator are exposed to ambient electromagnetic interferences, which can either be radiated or near-field coupled, as shown in Fig. 4. For radiated interferences, their sources are mainly from changing magnetic fields generated by nearby current-carrying conductors (not the measured primary current), electromagnets and/or permanent magnets. A simple method for canceling their effects is thus shown in Fig. 5(a) [14], where the usual Rogowski coil has been wound with wire clockwise on an air-core. However, at the end of the coil, the wire is returned anticlockwise along longitudinal axis of the air-core to the beginning of the coil. Two terminals can then be led out for an onward connection to an integrator. Doing so allows induced voltages in the return loop and coil, generated by the same radiated interferences, to cancel each other perfectly. It is therefore important to enforce the manufacturing precision of the return and coil in a high-end Rogowski current sensor.

As for near-field coupling, they are mostly associated with rapidly changing electric fields caused by nearby power semiconductor devices switching at high frequencies. Those rapid changes then induce spiky electrical noises to leak through parasitic capacitances and parasitic inductances to the coil, which in turn, cause an erroneous high-frequency voltage component to appear across terminals of the coil. This erroneous voltage can be removed by adding a shield to enclose the coil and its return, like in Fig. 5(b) [24], [25]. It is thus possible to avoid influences from electromagnetic interferences, even though their sources of generation are practically impossible to eliminate.

IV. PROGRESSION FROM HELICAL TO PCB ROGOWSKI COIL WITH RETURN LOOP

Earlier illustrations in Figs. 1 and 5 have mostly drawn the Rogowski coil as a helical coil, which indeed has been a popular structure for implementing small flexible current probes [14]. Further size reduction for better integration with a power semiconductor device has however prompted its redesign as a coil inside a multilayer PCB. The coil now consists of traces and vias, and has a less symmetrical rectangular cross section for its turns, as compared to the circular cross section of a helical coil.
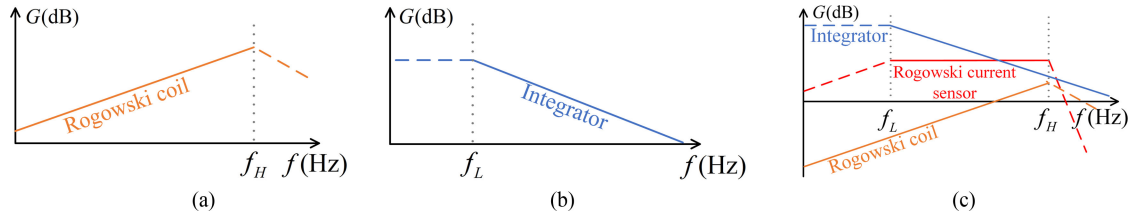
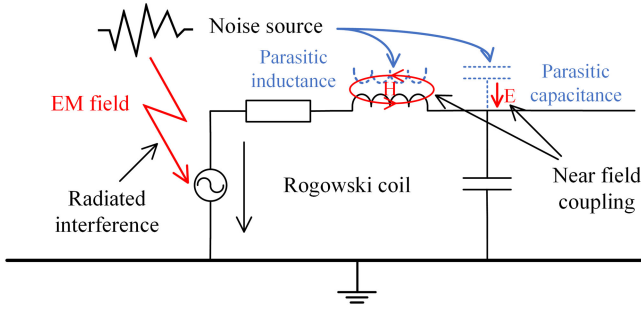Fig. 3. Frequency characteristic of (a) Rogowski coil, (b) integrator, and (c) Rogowski current sensor.

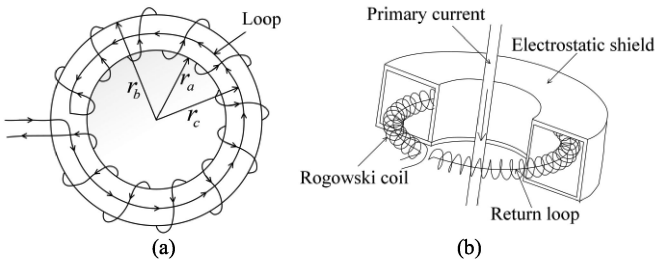Fig. 4. Radiation interference and near-field coupling when applying a Rogowski coil.

Fig. 5. Structure of (a) return loop and (b) electrostatic shield.
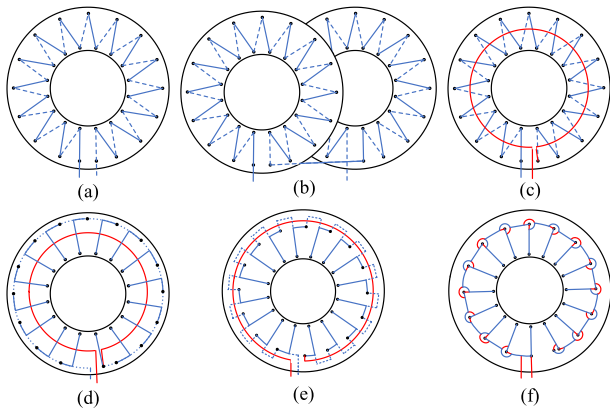

Fig. 6. Different design of PCB Rogowski. (a) Ordinary wiring. (b) Ordinary wiring with two PCBs. (c) Ordinary wiring with return loop. (d) New wiring with return loop. (e) Improved wiring with return loop. (f) Promising wiring.

More design issues must hence be addressed when implementing the PCB Rogowski coil with its accuracy and immunity toward external interferences retained. To illustrate, several classical coil layouts in Fig. 6 can be considered as examples.

Beginning with Fig. 6(a), the coil is formed by (solid blue) traces on the top layer and (dashed blue) traces on the bottom layer [26]. The top and bottom traces are then joined by vias between the two layers, marked as dots in the figure. Turns of the coil are thus rectangular in cross section. Despite that, the coil is still prone to radiated magnetic and conducted electric interferences, as explained in Section III-D. To improve its immunity toward the former, a second coil in another two-layer PCB can be placed very close to the first. However, as depicted in Fig. 6(b), directions of winding of the two coils must be different with one turning clockwise and the other anticlockwise. Erroneous induced voltages in the two coils caused by the same interfering magnetic fields then have the same magnitude, but opposite polarities. In other words, they cancel when finding total induced voltage across the two coils connected in series by a through-hole. Inclusion of two "opposing" coils for canceling interferences is thus a simple and effective technique, especially suitable for high-power applications. However, its cost is high, and its resonance frequency is low at only 5 MHz due to doubling of turns [17].

A second design has therefore been formulated, based on the concept of including a return loop, first introduced with the helical Rogowski coil in Fig. 5(a). The resulting structure however requires a multilayer PCB with at least four layers. The coil is again formed by top- and bottom-layer traces connected by vias, like in Fig. 6(a). However, unlike Fig. 6(a), Fig. 6(c) shows that the (dashed) end of the new coil has been connected to a (red) circular axial return routed on the inner layers. This return circles anticlockwise to the (solid) end of the coil, which together form the two output terminals of the coil. Ideally, the planar area enclosed by the return must be equal to that enclosed by the coil, but with the PCB implementation in Fig. 6(c), this is not achievable due to asymmetry between traces on the top and bottom layers. In other words, the coil axis no longer passes through centers of all turns, which hence renders the axial return to be less effective [27].

To solve the problem, a new layout for traces on the top and bottom layers has been tested in [28] and shown in Fig. 6(d). Although symmetry has now been restored, the new layout in Fig. 6(d) is still burdened by large errors caused by radiated magnetic interferences, according to tests done in [28]. The reason uncovered is magnetic flux area enclosed by the return loop is still not completely equal to the area enclosed by the coil despite its symmetry. Another improved layout has therefore been proposed to equalize both areas [28], as shown in Fig. 6(e). That layout works fine, but introduces complex computations
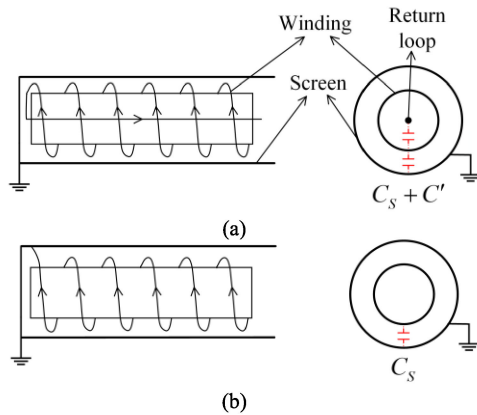
Fig. 7. Configurations for the screened coils. (a) Axial return. (b) Screen return.

Fig. 8. PCB Rogowski coil layer design on a (a) six-layer PCB and (b) four-layer PCB.

for finding the trace lengths, their diameters and separations on the top and bottom layers of the PCB. It is therefore not as simple to realize.

Subsequently, a promising coil layout has been proposed in [29] and shown in Fig. 6(f). Its purpose is to avoid complex computations by introducing a (red) return coil rather than a loop. The return coil routes along the same path as the main coil, but in the opposite direction. They therefore enclose the same planar areas. The idea is, in fact, like Fig. 6(b), but with both clockwise and anticlockwise coils neatly interlaced together in a single PCB. It is therefore a compact design that can promptly resist radiated magnetic interferences.

V. TRANSFERRING SHIELDING TECHNIQUES FROM HELICAL TO PCB ROGOWSKI COIL

Another source of noise influencing the measurement is near-field coupling introduced in Section III-D. An obvious approach to resist it is thus to add a shielding layer, which although effective, can introduce other tradeoffs. These tradeoffs must be understood, and they are hence described here for various shielding techniques that can be used with a PCB Rogowski coil.

A. Shielding Screen

Near-field coupling in the environment is mostly from nearby steep voltage changes or *du/dt*, which in spatially constrained power-electronic systems are very common because of their fast-switching semiconductor devices. These interferences can however be blocked from a Rogowski coil by inserting a shielding screen, as proven through experiments in [19]. More in-depth studies of the screen's effects have later been conducted in [30], using those two simple helical structures shown in Fig. 7. The knowledge developed can subsequently be transferred to a PCB Rogowski coil. In the meantime, Fig. 7(a) shows the first structure having both a shielding screen and a return along its inner center. Parasitic capacitances can therefore exist between the coil and its return, and between the coil and its screen. Together, they result in equivalent parasitic capacitance $C_S + C'$, whose undesired influence is to lower bandwidth of the coil.
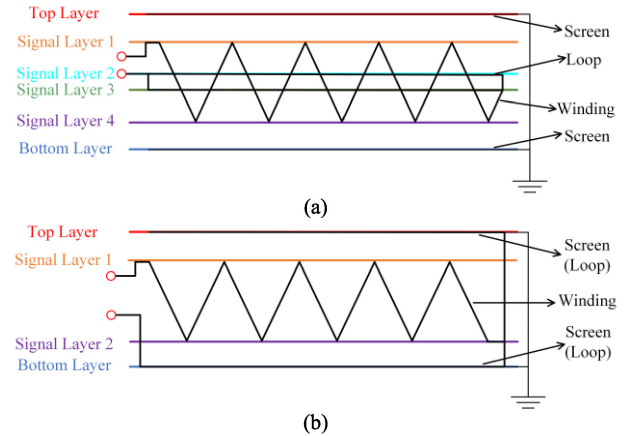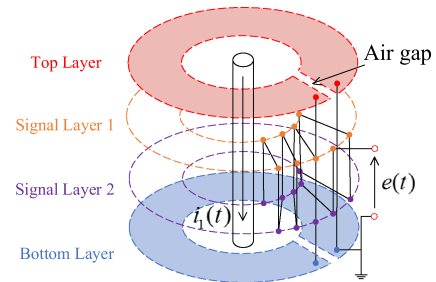

Fig. 9. Three-dimensional view of four-layer screen-return PCB Rogowski coil.

This parasitic can however be reduced by providing a return on the screen, in addition to its usual shielding function. The new parasitic capacitance is then only C_S, as marked in Fig. 7(b) showing the new structure known as an inverted coil.

A shielding screen can similarly be implemented with a PCB Rogowski coil having more than two layers. An example six-layer implementation is given in Fig. 8(a), where its screen planes, coil traces, and return traces are on its outermost, middle, and innermost two layers, respectively [23]. It therefore mirrors the helical structure shown in Fig. 8(a), and hence has a large parasitic capacitance and a small bandwidth. A cheaper and less complex alternative has then been tested in [31] using a four-layer PCB, as demonstrated in Fig. 8(b). An essential feature built into that structure is its screen on its outermost two layers must now serve as both a shield and a return for the coil routed on its innermost two layers. Such dual functionalities however require the screen to have an air-gap for explicitly directing the return.

An example planar view with the air-gap is given in Fig. 9, where it can be seen that the coil begins at its ingoing terminal and circles anticlockwise. At its end, the coil connects to the uppermost and lowermost shielding planes below the air-gap. The air-gap then forces the return to traverse clockwise (the intended opposite direction) along the shielding planes. Upon reaching their ends, both planes are connected and grounded. It is therefore possible for the shielding screen to
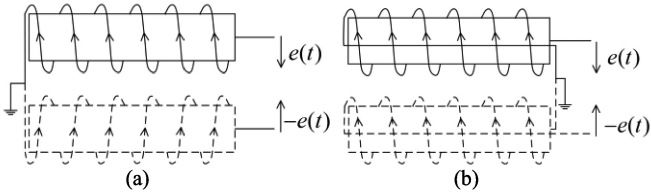
Fig. 10.　Two different structures of a differential Rogowski coil. (a) Wound in opposite directions. (b) Wound in the same directions.

have dual functionalities and the Rogowski coil to have less layers with a smaller parasitic capacitance.

B. Implicit Shielding With Differential Coil

Another way to resist external du/dt interferences is to wind a differential Rogowski coil [32]. Two structures, easily demonstrated in helical forms, are shown in Fig. 10 [30], before identifying which can readily be used for PCB implementation. The first structure consists of two windings wound in opposite directions, as illustrated in Fig. 10(a). Their terminals on the left of the figure are then grounded, whereas their terminals on the right form differential output of the overall Rogowski coil. Likewise, the second structure in Fig. 10(b) uses two windings, but wound in the same direction. Each winding has an axial return, and the two windings can then be connected one after another, as depicted in Fig. 10(b). Such connection is however not in series, because of the grounded central tap, through which current can enter or leave the windings.

In either type, the two windings must be wound symmetrically, so that the same erroneous voltages appear across them, produced by the same unavoidable du/dt interferences. These voltages then cancel at the differential output of the Rogowski coil. Working principles of such differential coil [29], [33] can better be illustrated by Fig. 11, where $u_{\text{ext}}(t)$ represents a source of external du/dt interferences, C_P represents parasitic capacitance, and the others are coil parameters defined earlier in Fig. 2. Capacitance C_P should moreover not be confused with C_S. The former is for capacitive coupling with the noise source external of the coil, whereas the latter is for parasitic capacitance internal of the coil.

Irrespective of that, capacitive coupling current $i_{\text{couple}}(t)$ from the interfering source can then flow along the single loop marked in Fig. 11(a) for an ordinary Rogowski coil with only a single winding. The flow changes to two current loops in Fig. 11(b), after adding a second winding to form a differential Rogowski coil. Since these loops point in opposite directions, their associated terminal voltages ideally oppose each other, even though they have the same magnitude notated as $u_{\text{couple}}(t)$ in the figure. They hence cancel at the output of the differential Rogowski coil measured from the top and bottom terminals in Fig. 11(b). In other words, only voltage $2e(t)$, induced by the desired primary current in the two windings, is sensed at the output of the Rogowski coil.

The same differential concepts in Fig. 10 can now be transferred to a PCB Rogowski coil. But, between the two structures, the one in Fig. 10(a) is likely to be preferred since it can be implemented with the PCB layout shown in Fig. 6(f)
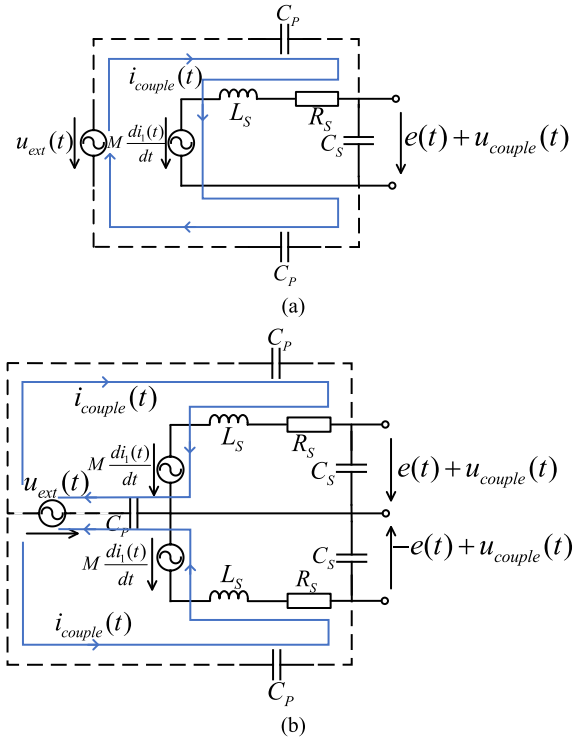
Fig. 11.　Effect of capacitive coupling. (a) Ordinary winding. (b) Differential winding.
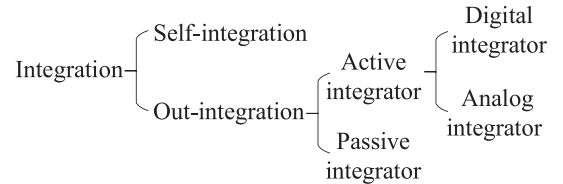
Fig. 12.　Classification of the integrator in a Rogowski coil.

and described at the end of Section IV. The obtained differential coil can then block both radiated magnetic and du/dt interferences simultaneously. The only limitation is, with many turns for forming the two windings, self-inductance and parasitic capacitance of the overall coil are high. The bandwidth of the coil for measurement will hence be compromised, which presently is still an issue yet to be resolved.

VI. PROSPECTIVE INTEGRATORS

As explained in Section III-A, the implemented Rogowski coil must connect to an integrator for recovering the primary current. Some prospective integrators are thus reviewed here, following the classifications depicted in Fig. 12.

A. Self-Integration

Self-integration relies on internal reactive components of the Rogowski coil. Externally, it requires only a noninductive resistor r connected to the terminals of the coil, as depicted in Fig. 13. By carefully ensuring that $r \ll 1/(\omega C_S)$, C_S can then be ignored, and by sizing $r \ll \omega L_S$, output of the integrator

Fig. 13. Self-integrator network.

Fig. 14. *RC* integrator. (a) Equivalent circuit. (b) Frequency characteristic.

versus the primary measured current can be expressed as [34]

$$\frac{U_{\text{OUT}}}{I_1} \approx j\omega M \frac{r}{j\omega L_S} = \frac{Mr}{L_S} = \frac{r}{N}(L_S \approx NM). \quad (2)$$

The sensing gain is thus a constant with value r/N, and the sensing bandwidth is infinite. Self-integration therefore appears to be suitable for measuring short current pulses a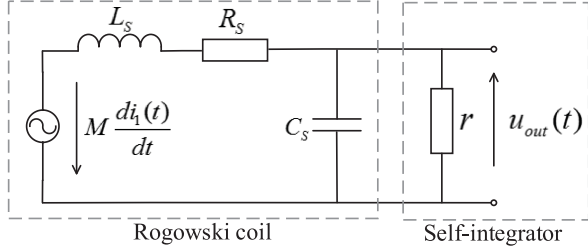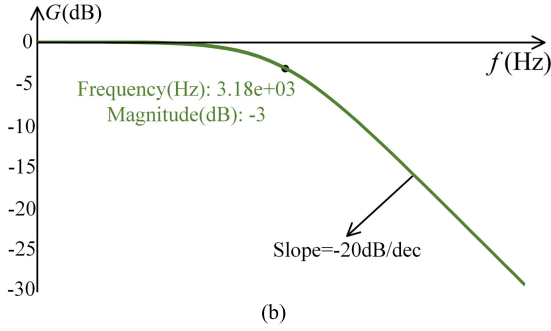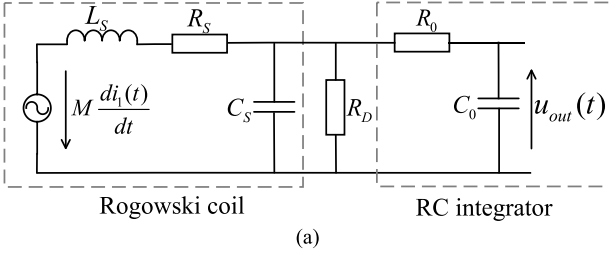nd/or high-frequency current variations. However, since $r \ll \omega L_S$, its sensing gain is very small and its output signal is very weak. Measurement with self-integration is thus prone to errors. Moreover, with r smaller than the characteristic impedance of the coil, impedance mismatch can happen, which sometimes can trigger apparent oscillations at the coil resonance frequency [22]. Self-integration is therefore not suitable for a Rogowski current sensor.

B. Passive RC Integration

The simplest passive integrator consists of only a resistor and a capacitor, or simply an *RC* integrator or filter, as shown in Fig. 14(a). Between the integrator and coil, a parallel resistor R_D can also be added, whose purpose is to match the output impedance of the coil with the input impedance of the integrator, so as to prevent unwanted coil oscillations [22]. It will however not affect the frequency characteristics of the *RC* integrator
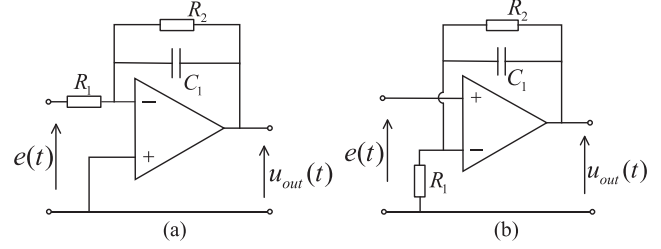

Fig. 15. Two kinds of integrators. (a) Inverting integrator. (b) Noninverting integrator.

plotted in Fig. 14(b). Assuming now that $R_0 = 50\,\text{k}\Omega$ and $C_0 = 1$ nF as some typical values, cutoff frequency of the *RC* integrator can be computed as

$$f_0 = \frac{1}{2\pi R_0 C_0} = 3.18 \times 10^3 \text{ Hz.} \quad (3)$$

In other words, integration can only be performed with high-frequency signals above 3.18 kHz. Below that threshold, the integrator degrades to only a trivial constant gain, smaller than unity. The depicted *RC* integrator therefore has a constrained usable range, dependent on the passive component values available for selection [35].

C. Active Analog Integration

Unlike passive integration, an external active integrator is less prone to variations of component values and termination at its output. Such improvement is possible because of at least one analog operational amplifier (op-amp) included in the active integrator. The included op-amp can either be of the inverting or noninverting type. With the inverting type, both input and feedback signals of the op-amp are at its negative input terminal, according to Fig. 15(a). Between this negative terminal and its output, an integrating capacitor C_1 and a large resistor R_2 in parallel are normally inserted. The purpose of R_2 is to limit the low-frequency gain, which if not constrained, can excessively amplify the low-frequency noise and saturate the integrator. Moreover, with an inverting op-amp, unwanted ringing and preshoot can happen, which in some instances can distort its output waveform, making it no longer similar to the measured primary current [34].

As for the noninverting integrator, its input is at the positive terminal of its op-amp, as shown in Fig. 15(b) [34]. Frequency response of this noninverting integrator can be plotted with $R_1 = 5\,\text{k}\Omega$, $C_1 = 1$ nF, and $R_2 = 511\,\text{k}\Omega$ as typical values. In practice, these values should additionally have small tolerances, in order to give an accurate measurement. For C_1, its value should also not be too large to preserve stability at high frequency. The chosen values can then be substituted to transfer functions derived in the following for the noninverting integrator for analysis:

$$\frac{U_{\text{out}}(s)}{E(s)} = \frac{R_1 R_2 C_1 s + R_1 + R_2}{R_1 R_2 C_1 s + R_1} = \frac{R_1 + R_2}{R_1} \cdot \frac{\frac{R_1 R_2 C_1 s}{R_1 + R_2} + 1}{R_2 C_1 s + 1}. \quad (4)$$
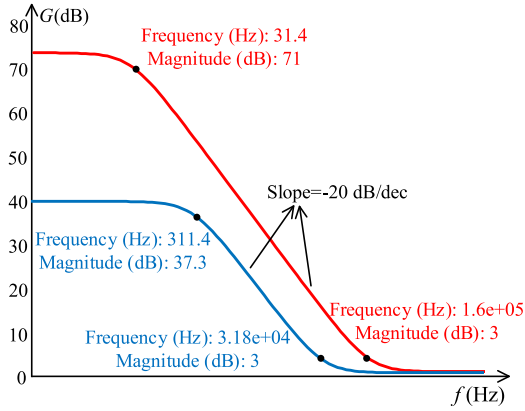
Fig. 16. Frequency characteristic of the active integrator.

Fig. 17. Combinatorial integrator with high bandwidth.

Also, as mentioned above, the value of R_2 is much larger than R_1, which in turn permits (4) to be simplified as

$$\frac{U_{\text{out}}(s)}{E(s)} \approx \frac{R_2}{R_1} \cdot \frac{R_1 C_1 s + 1}{R_2 C_1 s + 1}. \tag{5}$$

The final obtained characteristic of the noninverting integrator can then be drawn as the bottom (blue) curve in Fig. 16, which obviously proves that integration can be performed on signals with frequencies in the range of $f_1 < f < f_2$, where

$$f_1 = \frac{1}{2\pi R_2 C_1} = 311.4 \text{ Hz}, \ \ f_2 = \frac{1}{2\pi R_1 C_1} = 3.18 \times 10^4 \text{ Hz}. \tag{6}$$

Implicitly, (6) also informs that the range of integration can be widened by increasing R_2 and/or decreasing R_1. For example, a second (orange) characteristic with an enlarged range can be added to Fig. 16 for comparison. This broadened range is generally desirable, but it has somehow been compromised by a significantly increased low-frequency gain, which as mentioned earlier, can amplify the low-frequency noise and affect the measurement results. It is therefore not advisable to excessively widen the integration range of the noninverting integrator in Fig. 15(b). The noninverting integrator however has the advantage of drawing no current from its input, unlike the inverting integrator in Fig. 15(a) whose input current flows through all its resistances and capacitance. It is therefore much easier to insert another circuit, like a passive RC filter, at the input of the noninverting integrator. The resulting hybrid integrator avoids ringing and preshoot problems, because of an absence of capacitive coupling to its output. More details about such hybrid integrator are given in Section VI-E.

D. Digital Integration

Like most mathematic functions, integration can be performed digitally with an analog-to-digital converter (ADC) and a microprocessor, coordinated by an auxiliary control module [36]. The ADC is for digitizing the very small output voltage of a Rogowski coil, if it is not amplified by an external analog amplifier. Bit-resolution of the ADC must hence be high. Its common sampling rate with the microprocessor must also be much higher than the frequency of the input signal to retain
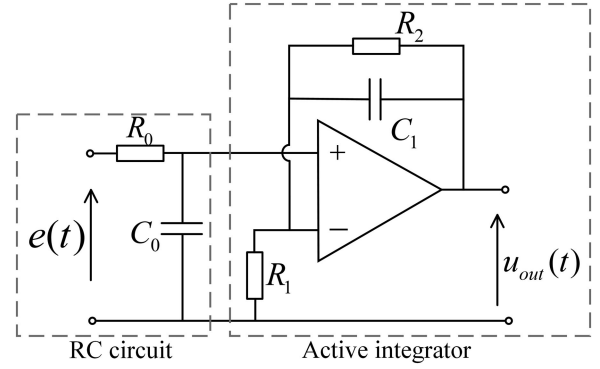
enough information for curve fitting. At times, this rate may additionally depend on the written integral codes, which commonly are based on the classical trapezoidal form of integration. Such numerical integration, with a nominal resolution of 16 b and a maximum sampling rate of 100k samples per second, usually offers a good compromise between computational time and accuracy [37].

Therefore, to summarize, the precision of a digital integrator depends on various factors, including its ADC resolution, computational speed of its microprocessor and extent of optimization built into its written integral codes. But, compared with most analog integrators, a digital integrator is generally less affected by mild high-frequency electromagnetic interferences, which in practice have been low-pass filtered off by the ADC, sample-and-hold, and other digital processes. Such low-pass filtering nonetheless narrows the bandwidth of the overall current sensor [38], [39], which undeniably is a tradeoff for power-electronic applications.

E. Hybrid Integration

Instead of separately, several integral techniques can be merged to form a hybrid integrator, whose characteristics better match operating specifications of the PCB Rogowski coil in a real working environment. For instance, in [34] and [35], a front-end passive RC integrator and a rear-end noninverting active integrator have been merged, as shown in Fig. 17. Their individual characteristics can be viewed from Fig. 14(b) with only a single cutoff frequency f_0 from (3), and Fig. 16 with two cutoff frequencies f_1 and f_2 from (6). Their merging can then be studied using Fig. 18, where (solid green and blue) piecewise linear representations of both individual characteristics have been included, together with the following important requirement:

$$R_0 C_0 = R_1 C_1. \tag{7}$$

Their resulting (solid red) piecewise linear magnitude response has also been plotted in the same Fig. 18, whose crossover frequency can be expressed as $f_c = f_0 = f_2$, because of the condition enforced by (7). It is hence clear that below f_c, integration is done by the noninverting active integrator, whereas above it, it is performed by the passive RC integrator. An indefinite extension of high-frequency integration and a smooth integral transition at f_c have therefore been enforced, so long as (7) is satisfied. Such enhancements are in addition to no increase
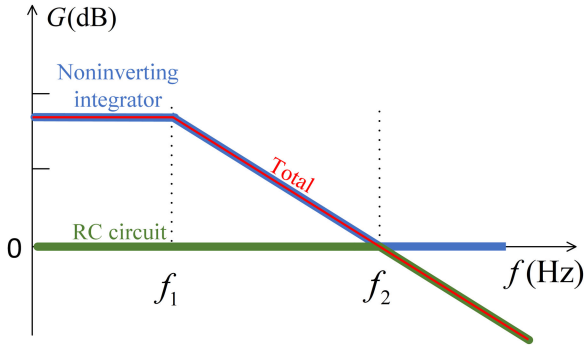
Fig. 18. Frequency characteristic curve.

of low-frequency gain below f_1. In other words, the hybrid integrator has better performances than the *RC* or noninverting integrator used alone, because of problems that the individual integrators face, as explained in the earlier two sections.

VII. COIL MODELING

Accurate parametric calculation has an important role in the exploration and design of Rogowski coils. For instance, the computed parameters can be substituted to an appropriately formulated coil model for predicting its performance, before actual implementation. The purpose of this section is thus to introduce some related lumped- and distributed-parameter models, together with their associated expressions for computing parameters. How these parameters can be measured in practice, especially if they cannot be easily calculated, has also been documented in an underlying section.

A. Lumped-Parameter Model

Lumped-parameter model of a Rogowski coil shown in Fig. 2 is the simplest and most used. It consists of a resistance R_S, a self-inductance L_S, a mutual inductance M, and a coil capacitance C_S. Equations for computing them are given in the following, with reference to dimensions of either a helical or PCB Rogowski coil [28], [40] marked in Fig. 19:

$$M = \frac{\mu_0 N w}{2\pi} \ln \frac{b}{a} \tag{8}$$

$$R_S = \rho_c \frac{l_w}{\pi d^2} \tag{9}$$

$$L_S = \frac{\mu_0 N^2 w}{2\pi} \ln \frac{b}{a} \tag{10}$$

$$C_S = \frac{4\pi^2 \varepsilon_0 (b+a)}{\log(\frac{b+a}{b-a})} \tag{11}$$

where
ρ_c resistivity of wire;
l_w length of wire;
d radius of wire;
w width of toroid;
N number of turns;
a, b inside and outside radii of coil.
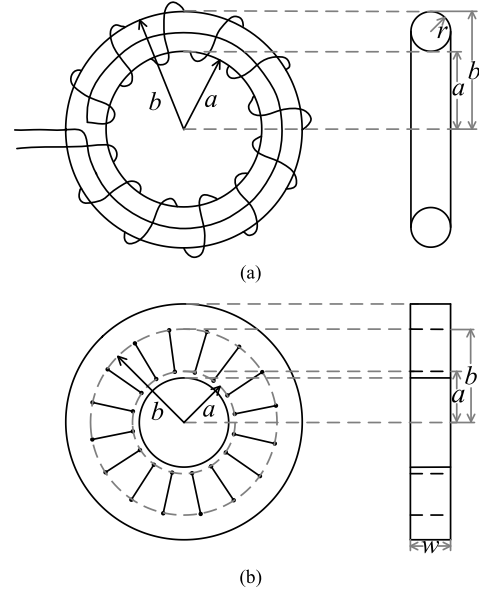
Fig. 19. Two kinds of dimension. (a) Flexible Rogowski coil. (b) PCB Rogowski coil.
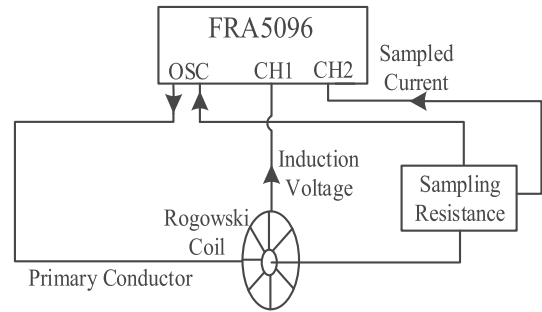
Fig. 20. Measuring layout for mutual inductance [28].

The above equations are however not practical since they do not consider skin and proximity effects at high frequencies [41]. Accuracy of the lumped-parameter model is therefore difficult to guarantee at high frequencies. At times, it may also be difficult to compute the parameters of the coil with satisfactory accuracy. Direct measurement, mostly with an impedance analyzer, may therefore be the only feasible technique. Parameters that can be measured with an impedance analyzer are internal resistance, self-inductance and lumped capacitance of the coil [28]. The measurements are usually accurate with a high-end analyzer. Alternatively, Shafiq *et al.* [42] proposed a less direct method, where parameters of the coil are found through capturing its frequency responses. The frequency, at which resonance occurs, can then be determined by fast Fourier transform, from which capacitance and inductance of the coil can be computed. Although such measurements appear complicated, other parameters, like capacitances of the probes and cables, can be determined (for compensation), in addition to self-impedance of the coil.

Another vital parameter to measure is mutual inductance of the coil, which in turn, determines its sensitivity. Mutual inductance should however be measured by a frequency-response analyzer, according to the measurement layout shown in Fig. 20

Fig. 21.   Distributed-parameter model of Rogowski coil.

TABLE II
LITERATURES OF ROGOWSKI COIL IN POWER ELECTRONICS

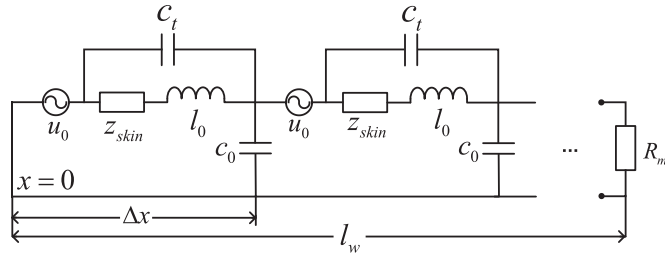| Year \ Object	MOS	IGBT	SiC MOS	GaN	Cap
1998		*[47]*[a]			
2006-2008	*[46]*[a]	[49] [51]			
2011-2012		[53] [45] [55]			[67]
2013-2014		[54]	[58]		
2015-2016	[29]	[48] [52] [56]	[60] [62]	*[36]*[a]	[69]
2017-2018		[50]	[23] *[57]*[a] [61]	*[63]*[a] [64] [65] [66]	[68]
2019			[31] [59]		

[a]References in italic are for the flexible Rogowski coil.

[28]. The principle is to set the sampling resistance to 1 Ω so that the sampled signal becomes equal to the primary current. The ratio of induced voltage to sampled signal (CH1/CH2 in Fig. 20) then gives mutual inductance of the coil. This measurement, together with those discussed above, however requires expensive equipment, which may not always be available. Therefore, where possible, it is generally preferred to formulate expressions for computing parameters of the coil, even with significant simplifications assumed.

B. Distributed-Parameter Model

Like a transmission line, a lumped model may not be accurate enough, if the length of the coil is too long. A distributed model with multiple identical segments in cascade should hence be considered, as discussed in [43] and [44] for a helical Rogowski coil. An illustration of it is given in Fig. 21, where parameters of each segment, computed in per unit length, are defined as follows:

μ_0 induced voltage within each segment of length Δx;
z_{skin} internal impedance of distributed winding including its skin effect;
l_o self-inductance of winding;
c_0 parasitic capacitance formed by winding, screen, and return;
c_t parasitic capacitance between any two adjacent turns;
R_m resistance of measuring equipment.

Computations of these parameters are comparably more complex, as analyzed in [45] in both time and frequency domains, before verifying the results with measurements. The discussed distributed-parameter modeling method is however not easily transferred to a PCB Rogowski coil assembled with traces and vias. This is especially true in case of a PCB Rogowski coil with very few turns for measuring very high-frequency current.

Guillod *et al.* [45] have therefore proposed the partial element equivalent circuit method, which elementarily is a fast and accurate method for establishing circuit-field coupling. Alternatively, Hewson and Aberdeen [30] have proposed a method for computing self-inductance of the PCB Rogowski coil, which in the reference has been mentioned as the toughest to compute. The method relies on distributed computing of inductances contributed by individual tracks and vias, before piecewise summing them to find self-inductance of the coil. Results obtained have shown a promising increase in accuracy, even though estimation errors still exist. Continuing effort must therefore be devoted to modeling, especially for a PCB Rogowski coil with asymmetrical rectangular turns.

Meanwhile, the above modeling methods can still provide some rough guidelines for designing a PCB Rogowski coil, such as the selection of its number of turns. In general, more turns lead to a bigger mutual inductance M for amplifying induced voltage of the coil. The induced voltage is thus less affected by small interferences, and hence easier to detect. But, with more turns, self-inductance L_S and parasitic capacitance C_S of the coil increase, which collectively cause its bandwidth to drop. An optimal tradeoff must therefore be found through continuous innovation in modeling.

VIII. EXAMPLE APPLICATIONS

A Rogowski current sensor in a power-electronic system is normally for detecting immediate current through a power semiconductor device for protection or other purposes. The power device can be any of those summarized in Table II, together with their related Rogowski references and years found in the literature. Some of these references in italic are for the flexible helical Rogowski coil, even though the main theme here is PCB Rogowski coil. Those references nonetheless serve as valuable examples for comparison, to better project the amount of space saving achieved by a PCB Rogowski coil. The space saved and eventual compactness realized are especially important with next-generation wide-bandgap devices, whose main attractiveness is their fast operating speeds, and hence much smaller accompanied passive components. Further elaborations on this aspect for various types of power semiconductor devices are given as follows.

A. Measuring Current Through mosfet

Flexible helical Rogowski coil has been used in [46] for measuring current through a MOSFET. A diagram showing the setup with a thin Rogowski coil circling one terminal of a discrete MOSFET with ease is given in Fig. 22(a). Such connection, although highly flexible and with a high bandwidth for measurement, is not compact and secure enough for mounting in a moving electric vehicle, for example, which lately has experienced rapid development [15]. Because of that,
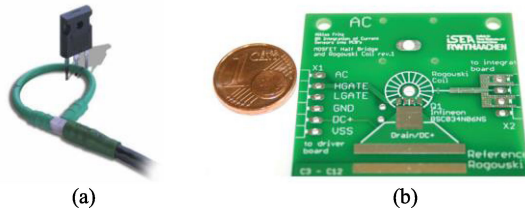
Fig. 22. Zoomed view of Rogowski coil measuring MOSFET current. (a) Flexible Rogowski coil [46]. (b) PCB Rogowski coil [29].
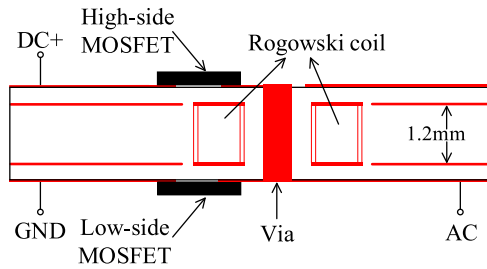

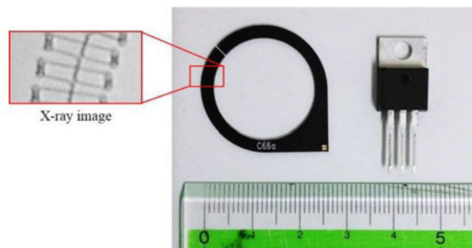Fig. 23. Model of the PCB board for coil [29].

Fig. 24. Photograph of the PCB-based Rogowski coil [50].

Fritz *et al.* [29] use a PCB Rogowski coil for measuring current through a MOSFET. Fig. 22(b) shows its actual implementation, which certainly is more densely packed and hence has a much smaller stray inductance [15], [16]. Fig. 23 further shows its design sketch, where the coil has been routed on the inner two layers of a four-layer PCB. The resulting coil has rectangular turns surrounding a thick via, drawn near the middle of the sketch. This via connects a high-side to a low-side MOSFET mounted on the top and bottom layers, respectively, to form a phase-leg. The via therefore carries pulsed current of either MOSFET, which as intended, induces an electromotive force in the Rogowski coil for measurement. Such measurement is likely more reliable, since it is read from a fixed coil, whose planar cross section is always perpendicular to the direction of current flow.

B. Measuring Current Through Insulated-Gate Bipolar Transistor (IGBT)

Using a Rogowski coil for measuring current through an IGBT has a relatively long history. Patented in 1998, it has been used in [47] for measuring current through the switch of an inverter. Subsequently, to improve reliability of the power module, Kogaa *et al.* [48] and Bortis *et al.* [49] have tried a PCB Rogowski coil for measuring current of an IGBT. An actual implementation of such a PCB Rogowski coil is given in Fig. 24. More embedding
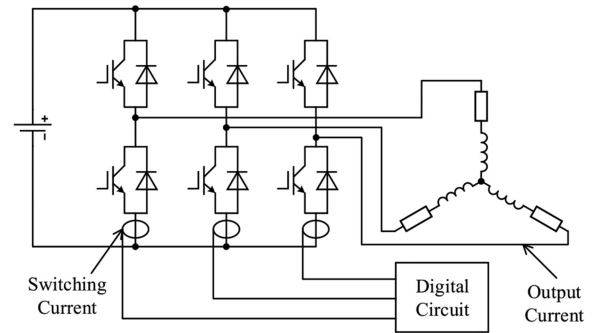

Fig. 25. Application of a three-phase inverter using Rogowski coil [50].
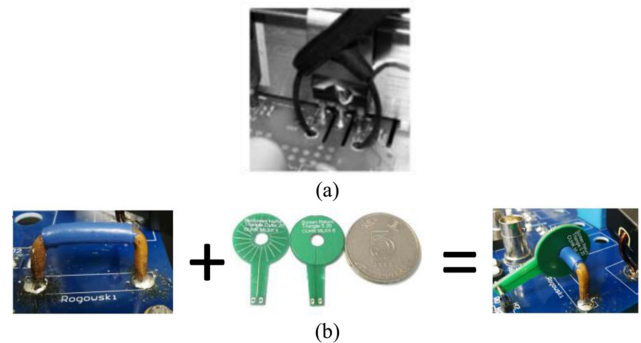
Fig. 26. Zoomed view of Rogowski coil measuring SiC MOSFET current. (a) Flexible Rogowski coil [57]. (b) PCB Rogowski coil [31].

has then been tried in [50], where a PCB Rogowski coil has been packed inside an IGBT module for measuring its pulsed current. Such measurement can be introduced to a three-phase inverter using multiple PCB Rogowski coils, as shown in Fig. 25. The measured switch currents, together with the modulation logics, can then be processed to restore the three-phase output currents for control without demanding extra output current sensors.

Other usages have also been mentioned in [51] and [52], where readings from the PCB Rogowski coils have been extracted for computing losses of the power devices. Alternatively, the sensed currents can be compared with a threshold for the rapid detection of overcurrents caused by short circuits. It is therefore a helpful way for protecting the IGBTs, as explained in [45] and [53]–[55]. Protection of the IGBTs may however not be the only objective. For example, in [56], *Texas Instruments* or *TI* has proposed the usage of PCB Rogowski coils for measuring phase currents of a three-phase induction motor drive. Its purpose is to detect a wide range of dynamic current conditions for protecting the motor against any short-circuit faults. It is therefore generally possible for the Rogowski coils to protect both the (motor) load and IGBTs (commonly used for implementing its drive).

C. Measuring Current Through SiC mosfet

With the development of fast-switching SiC MOSFET, the use of Rogowski coil for current measurement has become even more attractive, because of its unmatched high bandwidth and simplicity. Oyarbide *et al.* [57] have demonstrated the idea with a thin flexible Rogowski coil installed conveniently near the SiC MOSFET, as shown in Fig. 26(a). This is followed by Ming *et al.* in

Fig. 27. Second PCB Rogowski structure to measure SiC MOSFET current. (a) Side view. (b) Top view. (c) Fabrication drawing [58].
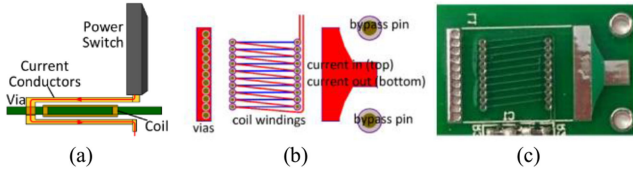
[31], where the small PCB Rogowski coil in Fig. 26(b) has been used instead with the SiC MOSFET. The structure in Fig. 10(b) is however not universal. For instance, a second PCB Rogowski structure has been mentioned in [58] and shown in Fig. 27, where the coil is now routed on a two-layer PCB, sandwiched between two (vertical) conductive traces carrying the current for measurement. This design has been claimed by its inventor to double the sensitivity of the coil, in addition to provide shielding to the coil by the two conductive traces.

Notwithstanding that, several Rogowski coils of either structure can be installed for measuring multiple switch currents of an inverter assembled with SiC MOSFETs. The switch currents can then be used for restoring output currents of the inverter [59]. Alternatively, the measured switch currents can be used for short-circuit protection of the SiC MOSFETs, rather than to depend on the long-established desaturation-detection technique. This is important because detecting desaturation works fine with Si IGBTs, but not with SiC MOSFETs, because of their different switching and output characteristics, as explained in [23]. Wang [23] has therefore suggested PCB Rogowski coils for protecting the SiC MOSFETs. The same idea has been mentioned in [60]–[62], where PCB Rogowski coil has again been tested to be ideal for short-circuit protection due to its high bandwidth, short response delay, high accuracy, small size, and low cost.

D. Measuring Current Through GaN Devices

GaN devices are newer generation of power devices with fast switching and high-temperature resistance. Their currents are typically measured to improve their switching performances. For that, Hain and Bakran [32] have proposed a helical Rogowski coil with differential windings for measuring the GaN switch current. Another helical Rogowski coil for measuring the GaN switch current has also been tried in [63] for subsequent realization of zero-crossing detection in an *LLC* converter. The trend has however gradually shifted to integrated PCB Rogowski coil with [64] introducing it for GaN short-circuit protection. Simulated and manufactured structures of that PCB Rogowski coil are given in Fig. 28 for demonstrating its small footprint. Even greater compactness with only a single-turn PCB coil has been mentioned in [65] for placement near to the power loop, so as to measure the GaN switch current accurately. This design is shown in Fig. 29(a), based on the same principle of measurement as other PCB Rogowski coils. But, with only a single turn, its bandwidth is incomparably high. Another breakthrough in bandwidth has also been demonstrated in [66] with its design shown in Fig. 29(b). That design has the Rogowski coil embedded within a laminated busbar in the PCB, whose test results show a
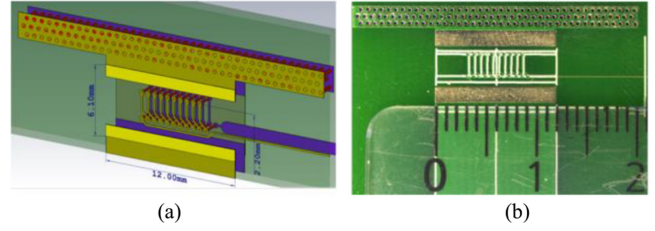
Fig. 28. PCB Rogowski coil for GaN short-circuit protection. (a) Simulated structure. (b) Manufactured structure [64].
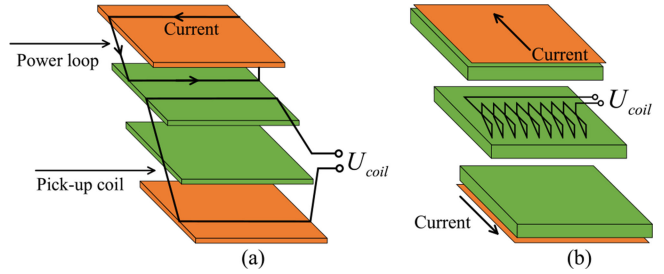
Fig. 29. Structure of compact PCB Rogowski coil. (a) Single-turn coil [65]. (b) Bus bar embedded coil [66].
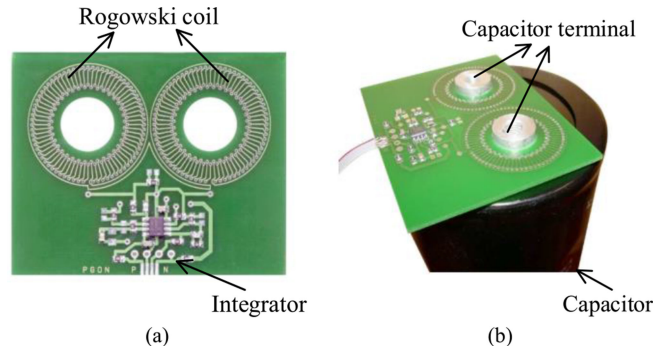
Fig. 30. PCB Rogowski coil for monitoring capacitor current. (a) Design of the coil. (b) Coil mounted on the capacitor [67].

bandwidth of about 100 MHz. It is thus suitable for measuring current through a GaN (or SiC) device, since it is higher than the 88 MHz computed in Section I.

E. Measuring Current Through Electrolytic Capacitor

Reliability of a power converter has become an important concern, as its applications broaden. One component, that is particularly vulnerable, is the electrolytic capacitor for forming the dc bus. Its current should hence be measured for identification of deterioration or fault. For that, the traditional approach is to insert a shunt for monitoring the capacitive current, but a shunt does not provide isolation. Its direct insertion may also cause problems during overcurrents and/or emergency shutdowns. Votzi *et al.* [67] have therefore suggested PCB Rogowski coil for monitoring current through the electrolytic capacitor. Fig. 30(a) shows the designed PCB Rogowski coil, whereas Fig. 30(b) shows how the coil can be easily connected to terminals of the electrolytic capacitor to help bring down the cost of measurement. The same measurement has also been tried in [68] and [69]

for evaluating lifetimes of their respective capacitors, in addition to detecting faults in switches. Those references have shown through experiments that with PCB Rogowski coils installed, reliabilities of their systems have improved without incurring expensive sensing costs.

F. Other Applications

Although the target of this review is PCB Rogowski coils in power-electronic systems, it can still be insightful to quote a few other systems for showing the wide usage of PCB Rogowski coils. For example, in [17], PCB Rogowski coils have been recommended for protecting power relays, because of their accurate measurements, flexibilities, and simplifications of a lot of wirings. Another application can be found in [70], where a PCB Rogowski coil has been installed for measuring ignition current in an automobile. Since this current directly reflects the pressure of a cylinder in the automobile, it can indirectly inform the state of the cylinder, which certainly is helpful. Besides, various PCB Rogowski coils have found relevance as a plasma current sensor [71], a transmission-line fault detector [72], and a motor-stator fault detector [73] to name only a few.

IX. CHALLENGES AND FUTURE TRENDS

Although PCB Rogowski coils have been employed in various applications, there are still some challenges to address, concerning its design and research, as explained in the following.

A. Finding a Precise Model for PCB Rogowski Coil

The cross section per turn of a PCB Rogowski coil is rectangular, rather than circular found in most helical Rogowski coils. Its area is thus defined by the length of traces and depth of vias forming each turn, rather than simply by a diameter. Both dimensions are independent, even though values for the depth are usually more restricted, determined by the PCB thickness and its number of layers. These differences, in addition to different parasitic effects from the trace and via, have made modeling of a PCB Rogowski coil more complex, which thus far, has only been tried by a few researchers. Precise modeling of a PCB Rogowski coil is thus urgently lacking, which if addressed, allows influences from various coil parameters to be studied. This can help to minimize the number of hardware prototypes implemented for testing.

B. Inventing Better Anti-Interference Techniques

Presently, blocking external interferences can be achieved by including a return and a shielding screen, or a second differential winding. Although both options are effective, they introduce large parasitic inductance and/or capacitance to the overall Rogowski coil. The outcome is a smaller resonance frequency, and hence a smaller derivative bandwidth for the coil. In other words, induced voltage at high frequencies cannot be produced accurately. Therefore, either a new anti-interference technique should be developed or an optimal design that resolves contradiction between shielding and bandwidth should be found.

C. Including DC and Low-Frequency Current Measurements

As explained in Section III-A, a Rogowski coil cannot measure dc and low-frequency currents. It is therefore necessary to include a second sensing technique, such as Hall-effect or magnetoresistive sensing, if low-frequency current measurement is mandatory. Two promising attempts can be found in [74] and [75], where they similarly tried to integrate a Rogowski and a Hall sensor into a single microchip. The resulting microsensor has a wide bandwidth, including dc, and is highly compact.

D. Improving Performance of Integrator

Several integrators have been reviewed in Section VI with the hybrid integrator identified as an appropriate choice due to its flexible tuning freedom and wide bandwidth. However, output drift of the integrator still exists, because of input offset error being integrated together with the incoming information. To reduce the drift and influences from low-frequency noises, a low-pass filter is essential in practice. However, the finite and limited gain of the low-pass filter at low frequencies causes waveform from the integrator to droop slowly. One recent solution is to use a pure integrator, with an electronic switch connected in parallel with its integrating capacitor, to eliminate the droop effect. The purpose of the switch is to reset the sensor output to zero at every switching period, so as to make the integrating output always follow the measured current. Resetting therefore works fine with solving the drift problem, but it generally increases the complexity of the integrator [23], [62]. An alternative simpler integrator with a large enough low-frequency gain, while retaining sufficient noise immunity, must therefore be invented.

E. Harmonizing Design of Rogowski Coil and Integrator

The highest frequency of measurement is usually limited by cutoff or resonance frequency of the Rogowski coil, if it is designed independently of the integrator (see Fig. 3). A better approach may be to dependently harmonize characteristics of the integrator and coil. The resulting bandwidth, assisted by an appropriate electronic circuit, may possibly extend beyond the resonance frequency of the coil. Harmonizing design of the coil and integrator should therefore be given some thoughts.

F. Designing PCB Rogowski Coils With Less Layers to Further Reduce Costs

The PCB structures introduced in Section V use either six or four layers to provide both return and screen for improving noise immunity. It may certainly be tough to further reduce to two layers, if only the coil is designed alone. It may however be feasible, if the coil is designed together with other components found in a power-electronic system. The resulting two-layer or even one-layer coil may then solely detect magnetic fluxes produced by the primary measured current with its noise immunity provided by other reinforced components.

X. Conclusion

This article presents a review of Rogowski coil with emphases placed on its progression from helical to PCB implementation and its power-electronic applications. From the latter, the general expectation drawn is that PCB Rogowski coil will continue to have relevance, especially with more power-electronic systems implemented with wide-bandgap devices. Its purposes are still to provide short-circuit protection, condition monitoring, loss computation and control in an unmatchable small footprint needed for building a compact power-electronic system. Despite that, there are still challenges to resolve, ranging from its structural design, anti-interference, packaging, signal processing to modeling. Particularly, with modeling, it is very tough to find a universal solution, since there are many different structures that a PCB Rogowski coil can assume. It is however very important to find a suitable model for studying influences from parameters of the PCB Rogowski coil, before physically implementing it. Many more years of research are therefore likely needed, before PCB Rogowski coil can be considered as a mature power-electronic component.

References

[1] F. Costa, P. Poulichet, F. Mazaleyrat, and E. Laboure, "The current sensors in power electronics, a review," *EPE J.*, vol. 11, pp. 7–18, 2001.

[2] S. Ziegler, "New current sensing solutions for low-cost high-power-density digitally controlled power converters," D.P. thesis, Dept. Elect. Comput. Eng., Univ. Western Australia, Perth, WA, Australia, 2009.

[3] ABCs of Probes, Tektronix Inc., 2013. [Online]. Available: https://www.tek.com/document/primer/abcs-probes-primer

[4] C2M0080120D, Silicon Carbide Power MOSFET, Cree, 2018. [Online]. Available: https://www.cree.com

[5] T. Asada, J. D. van Wyk, C. Xiao, W. G. Odendaal, and L. Zhao, "An overview of integratable current sensor technologies," in *Proc. Ind. Appl. Conf. Annu. Meeting Conf. Rec.*, Jan. 2003, pp. 1251–1258.

[6] L. Zhao, J. D. van Wyk, and W. G. Odendaal, "Planar embedded pick-up coil sensor for integrated power electronic modules," in *Proc. IEEE Appl. Power Electron. Conf.*, Feb. 2004, pp. 945–951.

[7] P. R. Palmer and C. M. Johnson, "Current measurement using compensated coaxial shunts," *IEE Proc.—Sci., Meas. Technol.*, vol. 141, pp. 471–480, Nov. 1994.

[8] Z. Zhang, B. Guo, F. F. Wang, E. A. Jones, L. M. Tolbert, and B. J. Blalock, "Methodology for wide band-gap device dynamic characterization," *IEEE Trans. Power Electron.*, vol. 32, no. 12, pp. 9307–9318, Dec. 2017.

[9] I. A. Metwally, "Self-integrating Rogowski coil for high-impulse current measurement," *IEEE Trans. Instrum. Meas.*, vol. 59, no. 2, pp. 353–360, Feb. 2010.

[10] S. Ziegler, R. C. Woodward, H. H. C. Iu, and L. J. Borle, "Current sensing techniques: A review," *IEEE Sensors J.*, vol. 9, no. 4, pp. 354–376, Apr. 2009.

[11] W. Li, C. Mao, and J. Lu, "Study of the virtual instrumentation applied to measure pulsed heavy currents," *IEEE Trans. Instrum. Meas.*, vol. 54, no. 1, pp. 284–288, Feb. 2005.

[12] W. Rogowski and W. Steinhaus, "Die Messung der magnetischen Spannung," *Elect. Eng.*, vol. 1, no. 4, pp. 141–150, 1912.

[13] A. P. Chattock, "On a magnetic potentiometer," *Proc. Phys. Soc. London*, vol. 9, no. 1, pp. 23–26, 1887.

[14] J. D. Ramboz, "Machinable Rogowski coil, design, and calibration," *IEEE Trans. Instrum. Meas.*, vol. 45, no. 2, pp. 511–515, Apr. 1996.

[15] A. Ostmann, T. Hofmann, C. Neeb, L. Boettcher, D. Manessis, and K. D. Lang, "Embedded power electronics for automotive applications," in *Proc. Int. Microsyst., Packag. Assem. Circuits Technol. Conf.*, Oct. 2012, pp. 163–166.

[16] C. Neeb, L. Boettcher, M. Conrad, and R. W. De Doncker, "Innovative and reliable power modules: A future trend and evolution of technologies," *IEEE Ind. Electron. Mag.*, vol. 8, no. 3, pp. 6–16, Sep. 2014.

[17] L. Kojovic, "PCB Rogowski coils benefit relay protection," *IEEE Comput. Appl. Power*, vol. 15, no. 3, pp. 50–53, Jul. 2002.

[18] R. Wang, S. Prabhakaran, W. Burdick, and R. Nicholas, "Rogowski current sensor design and analysis based on printed circuit boards (PCB)," in *Proc. IEEE Energy Convers. Congr. Expo.*, Sep. 2014, pp. 3206–3211.

[19] J. Hlavacek, R. Prochazka, M. Knenicky, K. Draxler, and R. Styblikova, "Influence of Rogowski coil shielding to measurement results," in *Proc. Int. Sci. Conf. Elect. Power Eng.*, May 2016, pp. 1–5.

[20] C. D. M. Oates, A. J. Burnett, and C. James, "The design of high performance Rogowski coils," in *Proc. Power Electron., Drives Conf.*, Apr. 2002, pp. 568–572.

[21] M. H. Samimi, A. Mahari, M. A. Farahnakian, and H. Mohseni, "The Rogowski coil principles and applications: A review," *IEEE Sensors J.*, vol. 15, no. 2, pp. 651–658, Feb. 2015.

[22] W. F. Ray and R. M. Davis, "High frequency improvement in wide bandwidth Rogowski transducers," in *Proc. Elect. Power Eng.*, 1999, pp. 1–9.

[23] J. Wang, "Switching-cycle control and sensing techniques for high-density SiC-based modular converters," D.P. thesis, Dept. Elect. Eng., Virginia Polytech. Inst. State Univ., Blacksburg, VA, USA, 2017.

[24] C. Hewson and W. R. Ray, "The effect of electrostatic screening of Rogowski coils designed for wide-bandwidth current measurement in power electronic applications," in *Proc. Power Electron. Spec. Conf.*, Jun. 2004, pp. 1143–1148.

[25] R.-Y. Han *et al.*, "Hybrid PCB Rogowski coil for measurement of nanosecond-risetime pulsed current," *IEEE Trans. Plasma Sci.*, vol. 43, no. 10, pp. 3555–3561, Oct. 2015.

[26] C. Wang, Y. Chen, G. Zhang, and Z. Zhou, "Design of printed-circuit board Rogowski coil for highly accurate current measurement," in *Proc. Int. Conf. Mechatronics Autom.*, Aug. 2007, pp. 3801–3806.

[27] Z. Yan and L. Hongbin, " The reliable design of PCB Rogowski coil current transformer," in *Proc. IEEE Int. Conf. Power Syst. Technol.*, Oct. 2006, pp. 1–4.

[28] T. Tao, Z. Zhao, W. Ma, Q. Pan, and A. Hu, "Design of PCB Rogowski coil and analysis of anti-interference property," *IEEE Trans. Electromagn. Compat.*, vol. 58, no. 2, pp. 344–355, Apr. 2016.

[29] J. N. Fritz, C. Neeb, and R. W. De Doncker, "A PCB integrated differential Rogowski coil for non-intrusive current measurement featuring high bandwidth and dv/dt immunity," in *Proc. Power Energy Student Summit*, 2015, Paper S05.2.

[30] C. Hewson and J. Aberdeen, "An improved Rogowski coil configuration for a high speed, compact current sensor with high immunity to voltage transients," in *Proc. IEEE Appl. Power Electron. Conf.*, Mar. 2018, pp. 571–578.

[31] L. Ming, Z. Xin, L. Wei, and P. C. Loh, "Structure and modelling of four-layer screen-returned PCB Rogowski coil with very few turns for high-bandwidth SiC current measurement," *IET Power Electron.*, vol. 13, pp. 765–775, 2020, doi: 10.1049/iet-pel.2019.0694.

[32] S. Hain and M. M. Bakran, "New Rogowski coil design with a high dV/dt immunity and high bandwidth," in *Proc. Eur. Conf. Power Electron. Appl.*, Sep. 2013, pp. 22–27.

[33] T. Funk and B. Wicht, "A fully integrated DC to 75 MHz current sensing circuit with on-chip Rogowski coil," in *Proc. Custom Integr. Circuits Conf.*, Apr. 2018, pp. 1–4.

[34] W. F. Ray and C. R. Hewson, "High performance Rogowski current transducers," in *Proc. IEEE Ind. Appl. Conf.*, Oct. 2000, pp. 3083–3090.

[35] J. A. J. Pettinga and J. Siersema, "A polyphase 500 kA current measuring system with Rogowski coils," *IEE Proc.—Elect. Power Appl.*, vol. 130, no. 5, pp. 360–363, 2013.

[36] E. Hemmati and S. Mohammad Shahrtash, "Digital compensation of Rogowski coil's output voltage," *IEEE Trans. Instrum. Meas.*, vol. 62, no. 1, pp. 71–82, Jan. 2013.

[37] G. D'Antona, M. Lazzaroni, R. Ottoboni, and C. Svelto, "AC current-to-voltage transducer based on digital processing of Rogowski coils signal," in *Proc. Sensors Ind. Conf.*, 2002, pp. 72–77.

[38] A. Marinescu and I. Dumbrava, "Validation of the software for digital processing of a Rogowski coil output signal," in *Proc. Int. Conf. Optim. Elect. Electron. Equip.*, May 2012, pp. 1189–1192.

[39] B. Djokić, "Calibration of Rogowski coils at power frequencies using digital sampling," *IEEE Trans. Instrum. Meas.*, vol. 58, no. 4, pp. 751–755, Apr. 2009.

[40] G. M. Hashmi, M. Lehtonen, and A. Ametani, "Modeling and experimental verification of covered-conductor for PD detection in overhead distribution networks," *IEEJ Trans. Power Energy*, vol. 130, no. 7, pp. 670–678, 2010.

[41] Y. Liu, F. Lin, Q. Zhang, and H. Zhong, "Design and construction of a Rogowski coil for measuring wide pulsed current," *IEEE Sensors J.*, vol. 11, no. 1, pp. 123–130, Jan. 2011.

[42] M. Shafiq, L. Kutt, M. Lehtonen, T. Nieminen, and M. Hashmi, "Parameters identification and modeling of high-frequency current transducer for partial discharge measurements," *IEEE Sensors J.*, vol. 13, no. 3, pp. 1081–1091, Mar. 2013.

[43] M. Xiang, H. Gao, B. Zhao, C. Wang, and C. Tian, "Analysis on transfer characteristics of Rogowski coil transducer to travelling wave," in *Proc. Int. Conf. Adv. Power Syst. Autom.Protection*, Oct. 2011, pp. 1056–1059.

[44] W. Stygar and G. Gerdin, "High frequency Rogowski coil response characteristics," *IEEE Trans. Plasma Sci.*, vol. PS-10, no. 1, pp. 40–44, Mar. 1982.

[45] T. Guillod, D. Gerber, J. Biela, and A. Muesing, "Design of a PCB Rogowski coil based on the PEEC method," in *Proc. Conf. Integr. Power Electron. Syst.*, Mar. 2012, pp. 1–6.

[46] C. R. Hewson, W. F. Ray, and R. M. Davis, "Verification of Rogowski current transducer's ability to measure fast switching transients," in *Proc. Appl. Power Electron. Conf. Expo.*, Mar. 2006, pp. 573–579.

[47] B. R. Pelly and P. V. Estates, "Current sensing circuit for pulse width modulated motor drive," U.S. Patent 5 815 391, Mar. 19, 1997.

[48] M. Kogaa, M. Tsukudab, A. K. Nakashimaa, and I. Omuraa, "Application-specific micro Rogowski coil for power modules—Design tool, novel coil pattern and demonstration," in *Proc. Int. Conf. Integr. Power Electron. Syst.*, 2016, pp. 459–462.

[49] D. Bortis, J. Biela, and J. W. Kolar, "Active gate control for current balancing in parallel connected IGBT modules in solid state modulators," in *Proc. Pulsed Power Plasma Sci.*, Jun. 2007, pp. 1323–1326.

[50] K. Hasegawa, S. Takahara, S. Tabata, M. Tsukuda, and I. Omura, "A new output current measurement method with tiny PCB sensors capable of being embedded in an IGBT module," *IEEE Trans. Power Electron.*, vol. 32, no. 3, pp. 1707–1712, Mar. 2017.

[51] L. Dalessandro, N. Karrer, M. Ciappa, A. Castellazzi, and W. Fichtner, "Online and offline isolated current monitoring of parallel switched high-voltage multi-chip IGBT modules," in *Proc. Annu. Power Electron. Spec. Conf.*, Jun. 2008, pp. 2600–2606.

[52] T. Krone, L. D. Hung, M. Jung, and A. Mertens, "On-line semiconductor switching loss measurement system for an advanced condition monitoring concept," in *Proc. Eur. Conf. Power Electron. Appl.*, Sep. 2016, pp. 1–10.

[53] A. Ahmed, L. Coulbeck, A. Castellazzi, and C. M. Johnson, "Design and test of a PCB Rogowski coil for very high dI/dt detection," in *Proc. Power Electron. Motion Control Conf. Expo.*, Sep. 2012, pp. 6–9.

[54] D. Gerber, T. Guillod, R. Leutwyler, and J. Biela, "Gate unit with improved short-circuit detection and turn-off capability for 4.5-kV press-pack IGBTs operated at 4-kA pulse current," *IEEE Trans. Plasma Sci.*, vol. 41, no. 10, pp. 2641–2648, Oct. 2013.

[55] D. Gerber, T. Guillod, and J. Biela, "IGBT gate-drive with PCB Rogowski coil for improved short circuit detection and current turn-off capability," in *Proc. Dig. Tech. Papers Int. Pulsed Power Conf.*, Jun. 2011, pp. 1359–1364.

[56] High Accuracy AC Current Measurement Reference Design Using PCB Rogowski Coil Sensor, Texas Instruments, 2016. [Online]. Available: http://www.ti.com/lit/ug/tidubv4a/tidubv4a.pdf

[57] E. Oyarbide, C. Bernal, and P. Molina-Gaudo, "New current measurement procedure using a conventional Rogowski transducer for the analysis of switching transients in transistors," *IEEE Trans. Power Electron.*, vol. 32, no. 4, pp. 2490–2492, Apr. 2017.

[58] Y. Xue, J. Lu, Z. Wang, L. M. Tolbert, B. J. Blalock, and F. Wang, "A compact planar Rogowski coil current sensor for active current balancing of parallel-connected silicon carbide MOSFETs," in *Proc. IEEE Energy Convers. Congr.*, Sep. 2014, pp. 4685–4690.

[59] S. Mocevic *et al.*, "Phase current reconstruction based on Rogowski coils integrated on gate driver of SiC MOSFET half-bridge module for continuous and discontinuous PWM inverter applications," in *Proc. IEEE Appl. Power Electron. Conf.*, Mar. 2019, pp. 1029–1036.

[60] J. Wang, Z. Shen, R. Burgos, and D. Boroyevich, "Design of a high-bandwidth Rogowski current sensor for gate-drive shortcircuit protection of 1.7 kV SiC MOSFET power modules," in *Proc. IEEE Workshop Wide Bandgap Power Devices Appl.*, Nov. 2015, pp. 104–107.

[61] S. Mocevic, J. Wang, R. Burgos, and D. Boroyevich, "Phase current sensor and short-circuit detection based on Rogowski coils integrated on gate driver for 1.2 kV SiC MOSFET half-bridge module," in *Proc. IEEE Energy Convers. Congr. Expo.*, Sep. 2018, pp. 393–400.

[62] J. Wang, Z. Shen, C. Dimarino, R. Burgos, and D. Boroyevich, "Gate driver design for 1.7 kV SiC MOSFET module with Rogowski current sensor for shortcircuit protection," in *Proc. IEEE Appl. Power Electron. Conf. Expo.*, May 2016, pp. 516–523.

[63] Z. Liu, R. Yu, T. Chen, Q. Huang, and A. Q. Huang, "Real-time adaptive timing control of synchronous rectifiers in high frequency GaN LLC converter," in *Proc. IEEE Appl. Power Electron. Conf. Expo.*, Mar. 2018, pp. 2214–2220.

[64] J. Walter, J. Acuna, and I. Kallfass, "Design and implementation of an integrated current sensor for a gallium nitride half-bridge," in *Proc. PCIM Eur.*, Jun. 2018, pp. 1–8.

[65] K. Wang, X. Yang, H. Li, L. Wang, and P. Jain, "A high-bandwidth integrated current measurement for detecting switching current of fast GaN devices," *IEEE Trans. Power Electron.*, vol. 33, no. 7, pp. 6199–6210, Jul. 2018.

[66] Y. Kuwabara, K. Wada, J. M. Guichon, J. L. Schanen, and J. Roudet, "Bus bar embedded Rogowski coil," in *Proc. IEEE Appl. Power Electron. Conf. Expo.*, Mar. 2018, pp. 2821–2826.

[67] H. L. Votzi, M. Vogelsberger, and H. Ertl, "Low-cost current sensor for power capacitors based on a PCB Rogowski coil," in *Proc. PCIM Eur.*, May 2011, pp. 621–626.

[68] E. Farjah, H. Givi, and T. Ghanbari, "Application of an efficient Rogowski coil sensor for switch fault diagnosis and capacitor ESR monitoring in non-isolated single-switch DC-DC converters," *IEEE Trans. Power Electron.*, vol. 32, no. 2, pp. 1442–1456, Feb. 2017.

[69] E. Farjah, T. Ghanbari, and H. Givi, "Switch fault diagnosis and capacitor lifetime monitoring technique for DC–DC converters using a single sensor," *IET Sci. Meas. Technol.*, vol. 10, no. 5, pp. 513–527, 2016.

[70] X. Xue, C. Xude, B. Xu, Z. Yuan, and G. Yu, "Design of auto cylinder pressure measurement system based on PCB planar Rogowski coil," in *Proc. Int. Conf. Meas., Inf. Control*, Aug. 2013, pp. 89–92.

[71] Q. Chen, X. Chen, Y. Deng, and H. B. Li, "PCB Rogowski sensor designs for plasma current measurement," in *Proc. Symp. Fusion Eng.*, Jun. 2007, pp. 17–21.

[72] X. Chu, X. Zeng, F. Deng, and L. Li, "Novel PCB sensor based on Rogowski coil for transmission lines fault detection," in *Proc. Power Energy Soc.*, Jul. 2009, pp. 1–4.

[73] T. Ghanbari and A. Farjah, "Application of Rogowski search coil for stator fault diagnosis in electrical machines," *IEEE Sensors J.*, vol. 14, no. 2, pp. 311–312, Feb. 2014.

[74] J. Jiang and K. Makinwa, "11.3 A hybrid multipath CMOS magnetic sensor with 210μTrms resolution and 3MHz bandwidth for contactless current sensing," in *Proc. Int. Solid-State Circuits Conf.*, Feb. 2016, pp. 204–205.

[75] T. Funk, J. Groeger, and B. Wicht, "An integrated and galvanically isolated DC-to-15.3 MHz hybrid current sensor," in *Proc. Appl. Power Electron. Conf. Expo.*, Mar. 2019, pp. 1010–1013.

Yafei Shi (Student Member, IEEE) was born in Hebei, China, in 1996. He received the B.S. degree in electrical engineering from the Harbin University of Science and Technology, Harbin, China, in 2018. He is currently working toward the master's degree in electrical engineering with the Hebei University of Technology, Tianjin, China.

His research interests include Rogowski current sensor and wide-bandgap devices.

Zhen Xin (Member, IEEE) received the B.S. and M.S. degrees from the College of Information and Control Engineering, China University of Petroleum, Qingdao, China, in 2011 and 2014, respectively, and the Ph.D. degree from Aalborg University, Aalborg, Denmark, in 2017.

In 2016, he was a Visiting Scholar with the University of Padova, Padova, Italy. From 2017 to 2018, he was a Postdoctoral Research Fellow with The Chinese University of Hong Kong, Hong Kong. Since 2018, he has been with the Hebei University of Technology, Tianjin, China, as a Professor. His research interests include condition monitoring of WBG-based power-electronic systems, modeling and validation of power electronic component failure mechanisms, and modeling and control of power converters for renewable energy systems.

Poh Chiang Loh received the B.Eng. (hons.) and M.Eng. degrees from the National University of Singapore, Singapore, in 1998 and 2000, respectively, and the Ph.D. degree from Monash University, Melbourne, Vic, Australia, in 2002, all in electrical engineering.

From 2013 to 2015, he was a Professor with Aalborg University, Aalborg, Denmark. Since 2015, he has been a Tenured Full Professor with the Chinese University of Hong Kong, Hong Kong, China. His research interests include power converters and their grid applications.

Frede Blaabjerg (Fellow, IEEE) received the Ph.D. degree from Aalborg University, Aalborg, Denmark, in 1992.

From 1987 to 1988, he was with ABB-Scandia, Randers, Denmark. He became an Assistant Professor in 1992, an Associate Professor in 1996, and a Full Professor of Power Electronics and Drives in 1998. His research interests include power electronics and its applications such as in wind turbines, photovoltaic systems, reliability, harmonics, and adjustable speed drives.

Dr. Blaabjerg was the recipient of 15 IEEE Prize Paper Awards, the IEEE PELS Distinguished Service Award in 2009, the EPE-PEMC Council Award in 2010, the IEEE William E. Newell Power Electronics Award 2014, and the Villum Kann Rasmussen Research Award 2014. From 2006 to 2012, he was an Editor-in-Chief for the IEEE TRANSACTIONS ON POWER ELECTRONICS. He was a Distinguished Lecturer for the IEEE Power Electronics Society from 2005 to 2007, and for the IEEE Industry Applications Society from 2010 to 2011. He was nominated in 2014 by Thomson Reuters to be between the most 250 cited researchers in engineering in the world.